Available online at www.sciencedirect.com
SCIENCE DIRECT®
Surface and Coatings Technology 184 (2004) 156–162
SURFACE & COATINGS TECHNOLOGY
www.elsevier.com/locate/surfcoat

On the surface preparation of nickel superalloys before CoNiCrAlY deposition by thermal spray

U. Bardi[a,*], L. Carrafiello[a], R. Groppetti[b], F. Niccolai[a], G. Rizzi[c], A. Scrivani[b], F. Tedeschi[b]

[a]*Consorzio Interuniversitario di Scienza e Tecnologia dei Materiali (INSTM), UdR Firenze, Polo Scientifico di Sesto Fiorentino, 50019, Sesto (Fi), Italy*
[b]*Dipartimento di Ingegneria Industriale, Università di Parma, Parma, Italy*
[c]*Turbocoating SpA, Rubbiano di Solignano, Parma, Italy*

Received 16 April 2003; accepted in revised form 24 October 2003
Available Online 27 February 2004

Abstract

This work is dedicated to the study and the characterization of the surface of nickel superalloys before the deposition of the MCrAlY (M=Co, Ni or both) bond coat. Our aim is to determine the factors (roughness, contamination and others) that lead to the best properties of the coating in terms of adhesion. We used MAR M247 samples as substrates. Different preparation treatments were considered: dry and wet blasting by corundum with different grain size distribution, dry blasting by silicon carbide and cleaning by solid carbon dioxide. In general, we observed that the highest roughness led to the best adhesion as measured by critical load tests. However, this parameter must be balanced against known problems related to the use of coarse abrasive powders.

Keywords: Plasma spray; Surface preparation; Thermal barrier coating; Bond coat; Blasting; MCrAlY

1. Introduction

The most commonly used structural materials for blades and other high temperature components of gas turbines are nickel superalloys such as MAR M247M, Inconel or Hastelloy. Thermal barrier coatings (TBCs) are widely used on these substrates as protection against high temperatures and oxidation. A TBC system consists of a top coat of yttria partially stabilized zirconia and an underlying bond coat (usually MCrAlY, where M is Ni, Co or a combination of both). MCrAlYs are normally deposited by thermal spray processes: air plasma spray, vacuum plasma spray or high velocity oxygen fuel [1,2]. In general, the adhesion of the whole thermal barrier system is strongly dependent on the surface preparation of the substrate and it is generally believed that a certain degree of roughness promotes better adhesion. However, a quantitative assessment of the effect of the roughness on adhesion, also in connection with other parameters such as contamination, has never been reported in the literature.

The present work is dedicated to the study of the surface preparation techniques of the nickel-based substrates before the deposition of the MCrAlY bond coat and their influence on the performance of TBC systems, with a special aim at determining the effects of such parameters as roughness and contamination. We considered different preparation processes: dry and wet blasting by corundum with different grain size distribution, dry blasting by silicon carbide and cleaning by means of solid carbon dioxide. The roughness and the morphology of the surface before and after these treatments were determined by 3D stylus profilometry. The hardness of the coating was measured by standard Vickers tests and the effect on the surface composition of the preparation process and of the heat treatment and transferred arc (TA) cleaning were studied by X-ray photoelectron spectroscopy (XPS) and by Auger electron spectroscopy (AES).

In a subsequent phase, the adhesion of the bond coat to the substrate was investigated by means of scratch

*Corresponding author. Tel.: +39-0554573118; fax: +39-0554573120.
E-mail address: bardi@unifi.it (U. Bardi).

0257-8972/04/$ - see front matter © 2003 Elsevier B.V. All rights reserved.
doi:10.1016/j.surfcoat.2003.10.135

Table 1
Details on the abrasive materials used for the tests

Surface preparation Technique	Abrasive material	Abrasive grain size
Dry blasting	Corundum	24 mesh
	Corundum	80 mesh
	Corundum	120 mesh
	SiC	220 mesh
Wet blasting	Corundum	24 mesh
Solid CO_2 cleaning	CO_2	Cylinders with 8 mm length and 3 mm diameter

testing. The results led to the identification of the optimum abrasive material grain size to enhance the adhesion of the bond coat to the substrate, and to understand the effect of the surface preparation on the mechanical and chemical properties of the bond coat.

2. Experimental

2.1. Sample preparation

MAR M247 metal samples were used as substrates for the present study in the form of plates of $100\times25\times6$ mm^3. The preparation techniques utilized were dry/wet blasting by corundum and silicon carbide using powders with different grain size distribution and solid CO_2 cryogenic cleaning [3]. Table 1 shows the grain size and the type of abrasive materials used for the tests.

The subsequent step to the abrasive treatment is preheating in order to remove contaminants such as moisture and volatiles. The samples were preheated in two steps, a first one in air at approximately 400 °C, and the second one in vacuum, where heating is combined with transferred arc (TA) cleaning in order to obtain a further removal of the contaminants. This latter treatment is also used to bring the substrates to the appropriate temperature for the deposition of the top coat.

After this procedure, the samples were coated with commercially available CoNiCrAlY powder (grain size distribution 25–45 μm) applied by low pressure plasma spray (LPPS) for a thickness of 300–400 μm. The final step was the thermal treatment at high temperature in vacuum (~1100 °C/2 h) in order to diffuse the coated layer and the substrate.

Summarizing, the cycle undergone by the samples was composed of the following steps:

- surface preparation by different abrasive materials,
- preheating in air and subsequently in vacuum,
- CoNiCrAlY deposition by LPPS,
- diffusion heat treatment in vacuum (~1100 °C/2 h).

After each treatment, the following tests were performed:

- evaluation of the surface morphology at the micrometric scale, with determination of 3D roughness parameters,
- determination of the surface composition by surface spectroscopies,
- adhesion evaluation by scratch test.

2.2. Analysis and testing

3D microscale measurements were performed by means of a three-dimensional digital stylus profilometer [4]. The 3D parameters obtainable by this method are based on the three-dimensional extension of 2D parameters defined in the ISO 4287 and DIN 4776 standards. The acquisition of the surface data is carried out by the scanning of a square area and sampling a 128×128 matrix of point with a resolution of 0.0250 mm for each step. The roughness parameters measured are the following:

Arithmetic mean deviation	S_a
Root mean square deviation	S_q
Ten point height	S_z
Maximum summit height	S_p
Minimum valley depth	S_m
Skewness of the surface	S_{sk}

XPS measurements were carried out using a standard XPS spectrometer in ultra-high vacuum and a conventional Al Kα radiation as X-ray source. The binding energy scale was calibrated with respect to the carbon 1s peak assumed to be at 284.8 eV. All the samples were pre-sputtered by a 3 KeV Ar^+ beam to eliminate removable contaminants, such as water or carbon. The quantification of the elemental concentration was carried out using the atomic sensitivity factors reported by Briggs and Seah [5]. AES measurements were performed in a different system using a standard AES system equipped with a cylindrical mirror analyzer and a 3-keV electron beam as primary excitation source. For both XPS and AES, the sampling depth can be estimated as of the order of 1–3 nm.

Standard Vickers hardness tests were performed in order to determine the effect of surface treatments, using a load of 500 g for 15 s of indentation time.

Table 2
Roughness values (μm) on samples dry blasted with corundum 24 mesh

	Raw material	After blasting	Preheating	TA
S_a	2.4±0.1	5.0±0.1	4.9±0.1	5.2±0.1
S_q	3.1±0.1	6.5±0.1	6.3±0.1	6.7±0.1
S_z	24.1±2.7	51.5±4.6	40.7±10.3	56.9±0.6
S_p	12.7±1.4	30.6±7.0	28.6±9.6	40.1±0.3
S_m	14.6±1.8	31.6±3.1	23.6±3.3	28.9±3.9
S_{sk}	−0.1±0.1	0±0.1	0±0.1	0±0.1

Table 3
Roughness values (μm) on samples wet blasted with corundum 24 mesh

	Raw material	After blasting	Preheating	TA
S_a	2.4±0.1	4.9±0.4	4.7±0.1	5.42±0.1
S_q	3.1±0.1	6.2±0.5	5.9±0.1	6.97±0.3
S_z	24.1±2.7	47.8±4.5	47.2±0.3	56.4±8.7
S_p	12.7±1.4	29.5±5.4	29.7±6.3	34.2±7.2
S_m	14.6±1.8	29.1±0.9	27.0±0	33.7±6.4
S_{sk}	−0.1±0.1	−0.1±0.1	−0.1±0.1	0±0.1

Table 4
Roughness values (μm) on samples dry blasted with corundum 80 mesh

	Raw material	After blasting	Preheating	TA
S_a	2.4±0	2.3±0.2	2.0±0.1	3.1±0.1
S_q	3.1±0	2.9±0.2	2.6±0.1	4.0±0.1
S_z	24.1±2.7	24.1±2.8	22.9±2.4	35.0±7.0
S_p	12.7±1.4	16.4±7.3	16.4±6.6	32.3±17.3
S_m	14.6±1.8	14.7±2.7	15.0±0.4	16.3±0.3
S_{sk}	−0.1±0.1	0±0.1	0±0.1	0±0.1

Table 5
Roughness values (μm) on samples dry blasted with corundum 120 mesh

	Raw material	After blasting	Preheating	TA
S_a	2.4±0.1	1.9±0.2	1.9±0.1	2.8±0.1
S_q	3.1±0.1	2.5±0.2	2.5±0.1	3.5±0.1
S_z	24.1±2.7	25.4±3.5	21.9±1.3	28.3±1.5
S_p	12.7±1.4	19.7±6.1	9.7±0.1	16.9±2.1
S_m	14.6±1.8	14.9±3.3	19.1±0.8	20.5±3.7
S_{sk}	−0.1±0.1	−0.4±0.2	−0.6±0.1	−0.2±0.1

Table 6
Roughness values (μm) on samples dry blasted with SiC 220 mesh

	Raw material	After blasting	Preheating	TA
S_a	2.4±0.1	1.6±0.3	1.6±0.3	1.9±0.1
S_q	3.1±0.1	2.0±0.3	2.1±0.3	2.5±0.2
S_z	24.1±2.7	15.6±3.0	11.9±3.6	21.3±2.0
S_p	12.7±1.4	8.1±1.8	7.1±1.3	12.0±3.7
S_m	14.6±1.8	11.0±2.9	8.5±3.1	16.7±6.5
S_{sk}	−0.1±0.1	−0.4±0.2	0.2±0.1	−0.4±0.4

Table 7
Roughness values (μm) on samples blasted with CO_2

	Raw material	After blasting	Preheating	TA
S_a	2.4±0.1	2.4±0.1	2.1±0.3	2.1±0.2
S_q	3.1±0.1	3.0±0.1	2.7±0.3	3.6±0.2
S_z	24.1±2.7	22.5±1.5	16.2±4.6	20.8±0.6
S_p	12.7±1.4	11.8±1.7	9.7±1.4	10.6±1.1
S_m	14.6±1.8	14.3±2.2	10.0±2.6	17.6±3.5
S_{sk}	−0.1±0.1	−0.2±0.1	−0.1±0.2	−0.3±0.1

The adhesion parameters were determined by means of scratch test measurements. In this test, a stylus is dragged across the surface of the coating to be tested under progressively increasing load. The load at which the removal of the coating occurs is taken as a measure of adhesion and it is termed critical load. Here, scratch tests were performed by a prototype apparatus developed on the same 3D geometrical analysis system mentioned earlier [4]. This instrument performs scratches under either progressively increasing or static load and acquires normal load, tangential force and acoustic emission. The stylus is fixed to the load-measuring device, while the specimen is placed on a sample-holder that is resting on load-measuring cells placed on a moving worktable. For all the tests reported here, the indenter was moved at a speed of 15 mm/min at a progressively increasing load at a rate of 65 N/min. The maximum scratch length was limited to 10 mm and the maximum load to 50 N.

3. Results and discussion

3.1. Geometrical evaluation

From the geometrical analysis at the micro-scale, it was possible to divide the preparation techniques in three main groups depending on their aggressiveness:

- Group 1 - dry and wet blasting 24 mesh: highest roughness (approximately double of that of the raw material).
- Group 2 - dry blasting 80, 120 e 220 mesh: medium roughness.
- Group 3 - cryogenic treatment and SiC blasting: no increase in the roughness with respect to the raw material.

Tables 2–7 show the 3D roughness parameters of all preparation techniques after each step of the working cycle (preparation, preheating in oven, TA in vacuum chamber) compared with the values of the raw material.

The main results that can be derived from this set of data is that the techniques that we defined as ‘group 1’ (high particle size blasting) considerably increase the roughness of the surface in comparison to the untreated substrate. The treatments defined as ‘group 2’ and ‘group 3’ do not increase roughness, on the contrary may slightly smooth the surface. These results can also be

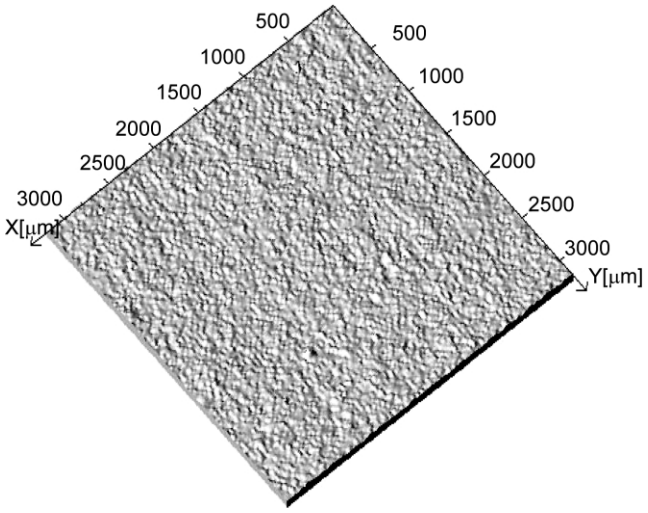

Fig. 1. Profilometric scan of the 'as-received' MAR M247 substrate.

shown in graphic form in the set of 3D profilometric scans shown in Figs. 1–4. The untreated substrate surface is shown in Fig. 1; data for the other treatments are shown in Figs. 2–4. The visual examination of the data confirms the interpretation of the tabulated results, which is only the first group of treatments that significantly increases the surface roughness.

The tabulated data also show that the surface roughness increases after treatment by TA on those surfaces previously blasted by corundum and silicon carbide. On the contrary, a treatment by TA decreases the roughness on the surface treated by dry CO_2. This could be explained because the TA is effective in removing residual abrasive particles embedded in the surface during the treatment.

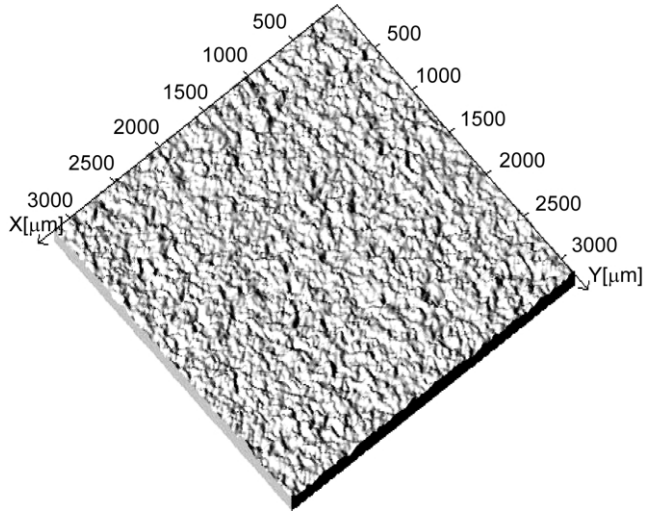

Fig. 2. Profilometric scan of the MAR M247 substrate after wet sandblasting with 24 mesh corundum.

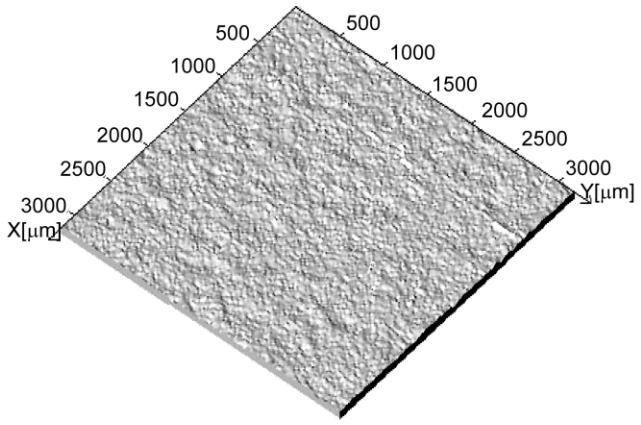

Fig. 3. Profilometric scan of the MAR M247 substrate after dry blasting with 80 mesh corundum.

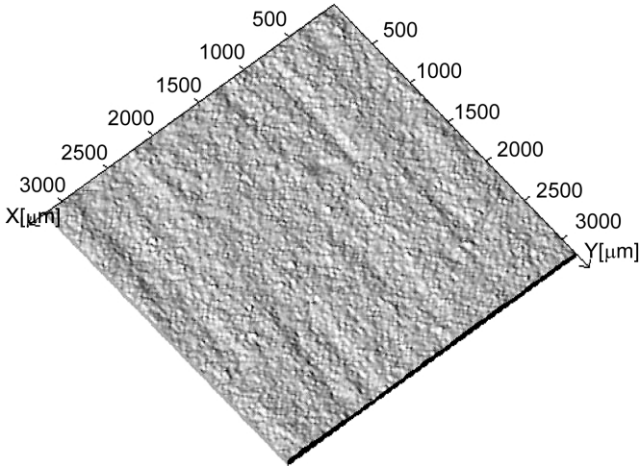

Fig. 4. Profilometric scan of the MAR M247 substrate after treatment with solid CO_2.

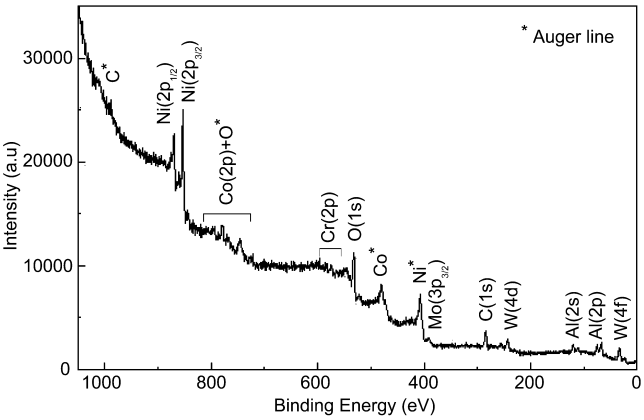

Fig. 5. Typical X-ray photoelectron spectrum (XPS) of the surface, in this case of an untreated MAR M247 substrate.

Table 8
XPS analysis of the sample dry blasted by corundum 24 mesh

Dry 24 mesh Elements	Atomic percentage		
	After blasting	Preheating	TA
Ni	16.48	4.15	26.04
Co	3.46	2.63	5.20
Cr	2.11	7.50	8.42
O	21.49	48.99	19.84
C	39.07	19.49	27.49
Al	14.31	16.47	8.57
W	3.08	0.77	4.45

Table 9
XPS analysis of the sample wet blasted by corundum 24 mesh

Wet 24 mesh Elements	Atomic percentage		
	After blasting	Preheating	TA
Ni	10.31	2.65	14.85
Co	4.87	1.03	3.18
Cr	3.29	3.09	4.88
O	19.52	34.90	32.20
C	50.12	44.19	29.70
Al	9.57	14.14	12.16
W	2.31	0.00	3.03

Table 10
XPS analysis of the sample dry blasted by corundum 80 mesh

Dry 80 mesh Elements	Atomic percentage		
	After blasting	Preheating	TA
Ni	11.46	3.55	10.46
Co	2.34	0.77	1.65
Cr	3.40	1.00	4.92
O	28.49	31.70	39.45
C	37.90	50.05	25.93
Al	14.31	12.82	15.27
W	2.09	0.11	2.31

Table 11
XPS analysis of the sample dry blasted by corundum 120 mesh

Dry 120 mesh Elements	Atomic percentage		
	After blasting	Preheating	TA
Ni	6.78	4.36	8.52
Co	1.36	1.30	1.67
Cr	1.61	5.53	3.90
O	21.92	46.35	44.71
C	58.02	27.53	22.02
Al	9.15	14.93	17.90
W	1.17	0.00	1.28

3.2. Surface composition measurements

Fig. 5 shows a typical XPS spectrum of an untreated MAR M247 metal strip. XPS spectra were also acquired for surfaces after the various treatments described before.

Table 12
XPS analysis of the sample dry blasted by corundum 220 mesh

Dry 220 mesh Elements	Atomic percentage		
	After blasting	Preheating	TA
Ni	10.91	2.47	3.93
Co	2.10	1.10	0.80
Cr	1.59	4.03	0.00
O	31.63	42.86	53.00
C	36.22	35.16	15.45
Al	15.40	14.15	26.16
W	2.15	0.24	0.66

Table 13
XPS analysis of the sample dry blasted by silicon carbide 220 mesh

SiC 220 mesh Elements	Atomic percentage		
	After blasting	Preheating	TA
Ni	8.64	10.60	18.62
Co	1.68	2.55	4.16
Cr	1.86	3.40	6.23
O	8.68	32.95	22.43
C	63.59	39.71	32.16
Si	11.44	5.15	5.10
Al	2.81	5.65	7.88
W	1.29	0.00	3.43

Table 14
XPS analysis of the sample blasted by frozen CO_2

Crio (CO_2) Elements	Atomic percentage		
	After blasting	Preheating	TA
Ni	15.60	4.31	24.37
Co	3.15	4.56	6.24
Cr	3.65	12.31	6.89
O	22.90	39.41	22.71
C	42.70	30.84	26.55
Al	8.65	8.23	9.23
W	3.36	0.34	4.00

The results of the elemental quantification are reported in Tables 8–14. From the data, it appears that at least in some cases the blasting process may contaminate the surface of the samples. For instance, for the case of samples sanded by silicon carbide, well detectable silicon and carbon signals can be observed. The preheating and cleaning treatments appear to be only partially effective in removing these elements. We observed that the O/Al ratio remained nearly constant for all the treated samples and larger than that for the untreated substrates, indicating that the blasting treatment is the main cause of contamination. Fig. 6 shows the Al and O atomic percentage for samples blasted by corundum: a higher level of contamination is evident for samples blasted by finer particles. Hence, better results can be

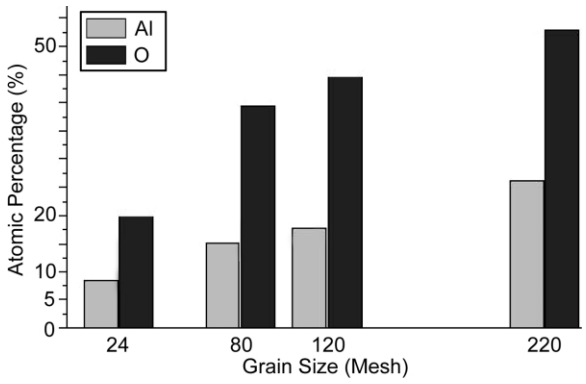

Fig. 6. XPS data analysis: oxygen and aluminium percentage of the samples dry sanded by corundum.

obtained using a medium or large sized particle in blasting.

During the preheating treatments, we normally observed that the percentage of aluminium and chromium increases, as measured by XPS. At the same time, the concentration of nickel, cobalt and tungsten decreases. This is due to the presence of residual oxygen in the atmosphere, which leads to the formation of aluminium and chromium oxides, as confirmed by the binding energy values we found for these elements. No evidence was found for the treatment resulting in the oxidation of elements other than chromium and aluminium in these conditions. TA treatments cause similar trends for all the samples, partially reversing the oxidation caused by the preheating treatment. In this case we observe by XPS a decrease in the concentration of chromium and aluminium and a parallel increase in the concentration of nickel, cobalt and tungsten.

The main results of these treatments from XPS measurements are summarized in Tables 8–14. Similar results were obtained by AES measurements. Typical XPS and AES spectra are shown in Fig. 5 and in Fig. 7.

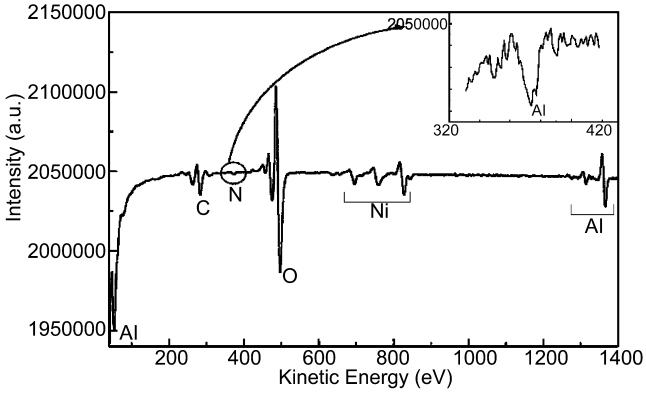

Fig. 7. Typical AES spectrum of the ‘as-received’ MAR M247 substrate.

Table 15
Microhardness values before and after the heat treatment

	Microhardness before Heat treatment ($HV_{0.5/15}$)	Microhardness after heat treatment ($HV_{0.5/15}$)
Dry 24	674 ± 46	554 ± 29
Dry 80	670 ± 43	525 ± 33
Dry 120	725 ± 39	558 ± 30
Wet 24	640 ± 26	508 ± 25
SiC 220	693 ± 32	547 ± 27
Cryo cleaning	750 ± 37	549 ± 27

3.3. Hardness and scratch tests

The results of the hardness measurements performed on the coatings before and after the heat treatment are shown in Table 15.

We note that the diffusion heat treatment decreases the overall average value of the hardness, but these values are similar for all the samples and are not affected by the surface preparation treatments.

Adhesion values were obtained as the ‘critical load’ measured by scratch tests for a selected number of samples chosen as follows:

– Group 1: dry blasting 24 mesh,
– Group 2: dry blasting 80 mesh,
– Group 3: CO_2 cryogenic cleaning.

Scratch testing was not applied to diffused samples because after the diffusion heat treatment the adhesion was too high to be measured. On each sample, the following tests were performed:

– optical microscopy evaluation of indentation,
– forces analysis,
– micro-geometrical analysis of indentations.

For all indentation tests, critical load (removal of the coating) occurred for all samples in the first 3 mm of length, i.e. under approximately 20 N. Before the critical point, the shape and depth of indentation are very similar for all samples: it seems that the preparation techniques do not affect the coating properties far away from the interface. With increasing load the indentation becomes more deep and defined: the lowest critical load was observed for samples treated by CO_2 cryogenic cleaning. Both optical microscopy and micro-geometrical analysis confirmed these considerations.

Table 16
Values of average critical load

Sample	Average critical load [N]
Dry 24 (group 1)	11.60 ± 0.8
Dry 80 (group 2)	10.46 ± 0.6
Cryo cleaning (group 3)	8.32 ± 0.3

The critical load measurements shown in Table 16 indicate that the 24 mesh dry blasted sample shows the highest resistance to scratching and results in the highest value of normal load.

4. Conclusions

The analysis carried out on different surface preparation techniques confirms that roughness is an important surface property affecting the adhesion of the bond coat to the nickel alloy substrate. Treatments with coarser particles produced less contaminated surfaces and a higher value of the coating adhesion to the substrate as measured from the critical load in scratch tests, at least before the diffusion treatment. On the other hand, the present work has not addressed the possibility that the use of coarse abrasive powder might generate high interface pollution due to voids and abrasive particles embedded in the substrate material. Such phenomena could impede effective coating/substrate inter-diffusion, and results in a poor adhesion after diffusion. Therefore, the optimal choice of the blasting parameters must take into account both the need to allow a good interdiffusion to get good metallurgical bonding as well as our find that higher roughness produces the best adhesion.

Acknowledgments

The authors acknowledge the assistance of Dr A. Rossi (Industrial Engineering Department, University of Parma). This work was supported by MIUR (Italian Research and University Ministry).

References

[1] R.B. Heimann, Plasma Spray Coating. Principles and Applications, VCH, Weinheim, 1996.
[2] Y. Tamarin, Protective Coatings for Turbine Blades, ASM International, Materials Park, OH, USA, 2002.
[3] Linde Gas Italia s.r.l., Pulizia a Getto con Ghiaccio Secco. Milano, 1999.
[4] P. Bracali, R. Groppetti, A. Scrivani, On a micro-topographic three-dimensional acquisition and analysis system for engineering surface characterisation, Proc. AITEM99, Brescia, Italy, 1999.
[5] D.M. Briggs, M.P. Seah, Practical Surface Analysis, John Wiley & Sons, New York, 1983.